Additive Manufacturing 7 (2015) 12–19

Contents lists available at ScienceDirect

Additive Manufacturing

journal homepage: www.elsevier.com/locate/addma

AlSi12 in-situ alloy formation and residual stress reduction using anchorless selective laser melting

Pratik Vora, Kamran Mumtaz*, Iain Todd, Neil Hopkinson

Centre for Advanced Additive Manufacturing, Department of Mechanical Engineering, University of Sheffield, UK

ARTICLE INFO

Article history:
Received 10 February 2015
Received in revised form 19 March 2015
Accepted 9 June 2015
Available online 12 June 2015

Keywords:
Additive Manufacturing
Selective laser melting
Residual stress reduction
In situ alloying
Aluminium alloys

ABSTRACT

Rapid melt pool formation and solidification during the metal powder bed process Selective Laser Melting (SLM) generates large thermal gradients that can in turn lead to increased residual stress formation within a component. Metal anchors or supports are required to be built in-situ and forcibly hold SLM structures in place and minimise geometric distortion/warpage as a result of this thermal residual stress. Anchors are often costly, difficult and time consuming to remove and limit the geometric freedom of this Additive Manufacturing (AM) process. A novel method known as Anchorless Selective Laser Melting (ASLM) maintains processed material within a stress relieved state throughout the duration of a build. As a result metal components formed using ASLM do not require support structures or anchors. ASLM locally melts two or more powdered materials that alloy under the action of the laser and can form into various combinations of eutectic/hypo/hyper eutectic alloys with a new lower solidification temperature. This new alloy is maintained in a semi-solid or stress reduced state throughout the build with the assistance of elevated powder bed pre-heating. In this paper the ASLM methodology is detailed and investigations into processing of a low temperature eutectic Al-Si binary casting alloy is explored. Two types of Al powders were compared; pre-alloyed AlSi12 and elemental mix Al + 12 wt% Si. The study established an understanding of the laser in-situ alloying process and confirmed successful alloy formation within the process. Differential thermal analysis, microscopy and X-Ray diffraction were used to further understand the nature of alloying within the process. Residual stress reduction was observed within ASLM processed elemental Al + Si12 and geometries produced without the requirement for anchors.

1. Introduction

Technologies such as Selective Laser Melting (SLM), Electron Beam Melting (EBM), and Direct Metal Deposition (DMD) etc. utilise metal powders as feedstock material to produce parts. SLM metal powders such as stainless steel, aluminium, titanium, nickel based alloys etc. are materials of interest within aerospace, medical and automotive industries etc. [1–4]. In recent years there has been a notable industry uptake of SLM and EBM technologies to manufacture end use parts. This is mainly a result of the processes' geometric freedom that is afforded to designers when manufacturing fully dense components from a variety of alloys. However the claim that SLM or EBM offers "unlimited" design freedom is untrue due to the requirement for supports/anchors that prevent certain geometries from geometrically distorting as a result of thermal residual stress. Further to this anchors are often costly, difficult and time consuming to remove. Because of the limitations anchors exert over the process, today efforts to limit the number of supports/anchors and minimise residual stress remains a major research priority.

2. Stress development and requirement for anchors/supports during SLM

During SLM processing, high heat intensities are generated by the laser source, this is required to ensure complete melting of metal powder particles and minimise part porosity [5,6]. However the rapid heating/melting of material is followed by a rapid solidification that induces thermal variations that cause areas of the scanned/processed layer to expand/contract at different rates, subsequently generating residual stress which can cause a component to geometrically distort/warp [5,7,8]. Anchors are metallurgically fused to the substrate plate and various locations across the laser melted component, forcibly holding geometries in place. Anchors are made from the same material as the SLM component and are also formed through the layer by layer melting of powder from the powder bed. An example of warpage and the required

* Corresponding author. Tel.: +44 01142227789.
E-mail address: k.mumtaz@sheffield.ac.uk (K. Mumtaz).

http://dx.doi.org/10.1016/j.addma.2015.06.003

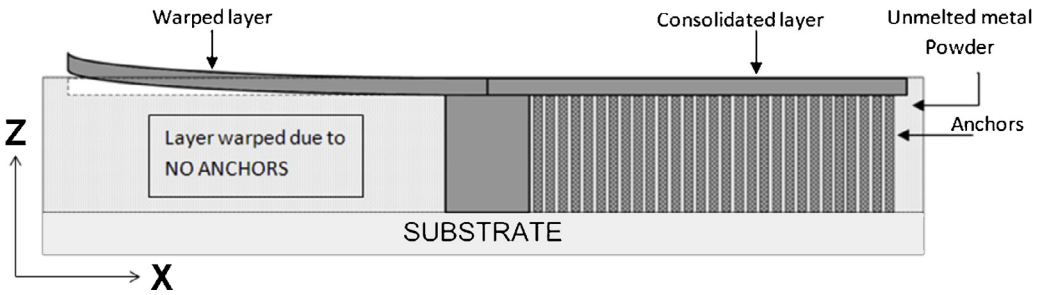

Fig. 1. Overhanging geometries most prone to warpage during SLM.

anchoring structure can be seen in Fig. 1. Typically large overhanging/unsupported geometries built parallel to the powder bed require the most support/anchoring [9].

An example of an un-anchored zinc SLM component can be seen in Fig. 2(a), the zinc part curls up due to it being un-anchored to the substrate, this type of warpage can be controlled with the use of anchors. Fig. 2(b) shows a steel (316L) SLM component made with and without anchors. The number and location of anchors are dependent on the part geometry and build direction/orientation [10]. However the inclusion of anchors does not guarantee a component will be warp free, large stress prone geometries can rip anchors from the substrate during a build causing it to fail. Once a build is complete the task of removing anchors adds time and cost to the build. This is particularly the case with cobalt chrome dental copings, crowns and bridges fabricated using SLM. These components require multiple support structures that later result in time-consuming surface finishing operations in order to preserve the dental surface integrity. In many cases the anchors cannot be accessed or removed, as a result the geometric freedom of the process is compromised as access is required to eventually remove these anchors. Even after anchor removal parts can still warp due to the remaining stress, this can be prevented by relieving the stress through furnace heating cycles prior to anchor removal [11].

The polymer AM process Laser Sintering (LS) uses lasers to process polymers from a powder bed. LS uses the same layer by layer fabrication method as SLM to produce parts but is able to do so without the requirement for anchors. LS uses special 'supercooling' polymers and careful processing temperature control to enable anchorless LS parts to be made [12]. LS materials nylon 11 and 12 (supercooling polymers) have re-freezing temperatures (138–143 °C) that are lower than their melting temperature (185–189 °C) [13]. During LS powder bed pre-heat temperatures are maintained above the material's solidification temperature but below its melting temperature [14], the laser scans regions of the powder bed causing the polymer to melt, more preheated powder is deposited and processed until the part is complete. The processed material is not given an opportunity to rapidly solidify but is instead held in a semi-solid/stress reduced state preventing part warpage. Materials that are not laser processed remain solid, whereas the bed temperature ensures that the laser melted polymer remains partially liquid throughout the build and does not transition back into a solid. After building, the part is allowed to cool over several hours and completely solidify. Eliminating rapid material solidification during a build reduces a component's tendency to warp and eliminates the requirement for anchors leading to greater geometric freedom and reduced post-processing operations. Furthermore, LS parts do not need to be physically attached to a substrate and therefore parts can be stacked on top of each other, increasing build volume within the process.

2.1. Eutectic alloy solidification characteristics

The super cooling behaviour of nylon 11 and 12 during LS processing allows parts to remain in a semi-solid state, stress reduced and removes the requirements for anchors. However, there are no known 'supercooling metals' in existence today that have a melt temperature that is significantly higher than the re-freezing temperature. However there are combinations of metals that when combined in specific proportions, form an alloy that has a lower solidification/freezing temperature than one or more of the individual materials prior to alloying. These alloys are known as 'eutectic alloy systems' with the lowest possible melting point forming the eutectic point [15].

Due to the low solidification temperature of eutectic compositions they are extensively used as soldering and casting alloys. Use of eutectic compositions minimise energy usage and alloy segregation during the casting process [16]. Eutectic systems form when alloying additions form a lowering of the liquidus lines from both melting points of the pure elements. At a specific composition there is a minimum melting point. A simple binary eutectic system is typified by the metallic alloy of bismuth and zinc. Pure elemental bismuth exhibits an equilibrium freezing point of 270 °C

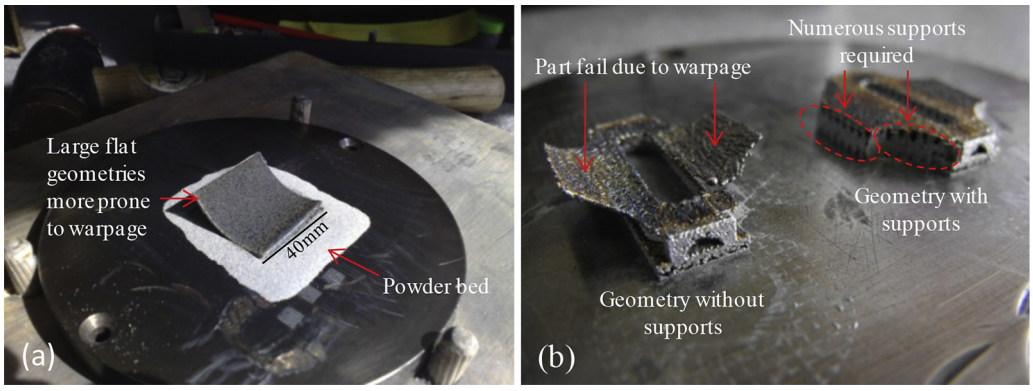

Fig. 2. Warpage of un-anchored zinc part (a) and un-anchored/anchored/steel geometry (b).

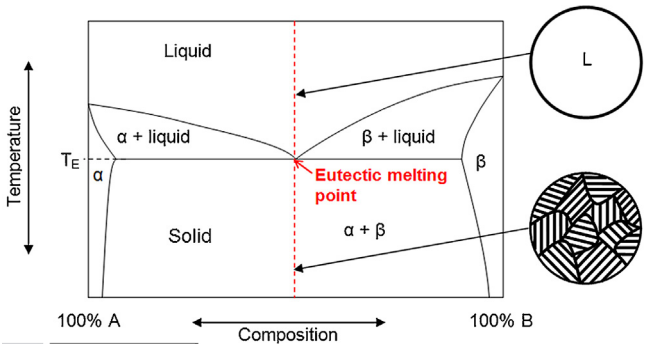

Fig. 3. Binary phase diagram containing material A and B.

and pure elemental zinc exhibits an equilibrium freezing point of 420 °C. When bismuth and zinc are fully alloyed in proportions of 97 wt% and 3 wt% respectively a melt point of 254 °C is formed, this is 16 °C lower than the melting point of bismuth [17]. A simple binary eutectic phase diagram is shown in Fig. 3. Alpha, beta, solid and liquid phases are shown with respect to varying material compositions and temperature, T_E represents the eutectic melting point. Eutectic material proportions can vary from the exact eutectic point creating hypo or hyper eutectics (alloys containing a eutectic system) with variable solidification temperatures and material properties. The range of compositions that have the potential to form eutectics is broad, ranging from aluminium alloys to higher temperature nickels.

2.2. Processing using Anchorless Selective Laser Melting

Removing or alleviating stress build up and the requirement for anchors within SLM can be achieved by preventing parts from completely solidifying during processing or maintaining in a stress reduced state. ASLM has been developed to prevent processed metal from completely solidifying during an SLM build [18]. This is achieved by forming a eutectic alloy or eutectic system (hyper/hypo eutectic) from two or more un-alloyed materials and maintaining powder bed pre-heating above the newly formed eutectic melting/solidification point. The following example demonstrates this method and is illustrated in Fig. 4; a batch of material A and B powder is mixed in their un-alloyed eutectic proportions (e.g. composition for eutectic melting point shown in Fig. 3). These materials are then deposited during the ASLM process while maintaining a bed temperature near to the eutectic point of the alloy but less than the melt temperature of the individual un-alloyed powder (to prevent melting and agglomeration of un-processed feedstock). It still may also be possible to pre-heat the powder bed to temperatures below the eutectic melt point so that stresses are not developed or are sufficiently relieved. Stresses can be sufficiently relaxed if the bed temperature allows diffusional relaxation of the material [19]. Dependant on the material, these relaxation kinetics are initiated between 40 and 60% of the solidification temperature of the material and above, this is also time dependant. When the laser scans regions of the powder bed the individual A and B powders will melt and form a eutectic alloy in-situ that will now only solidify at temperatures below the eutectic solidification point. Because the bed temperature is set near the eutectic point the melted/alloyed regions will not rapidly solidify or if within the diffusional temperature range will generate less stress than those formed during conventional SLM. Other eutectic compositions such as Al66Mg offer large processing windows of 212 °C (temperature difference between eutectic melt point and lowest melting point of individual un-alloyed material). A large processing window may be advantageous as the bed temperature control would not need to be regulated as precisely compared to that of a small processing window. Further to this a large processing window may reduce unwanted solid state sintering of unprocessed powders due to pre-heat temperature being far lower than the melt temperature of the un-alloyed material. This solid state sintering or "caking" of material causes material deposition issues due to agglomeration.

2.3. Aluminium and in situ alloying

There is a wide interest in processing aluminium alloys using SLM to produce complex parts with improved design. Aluminium

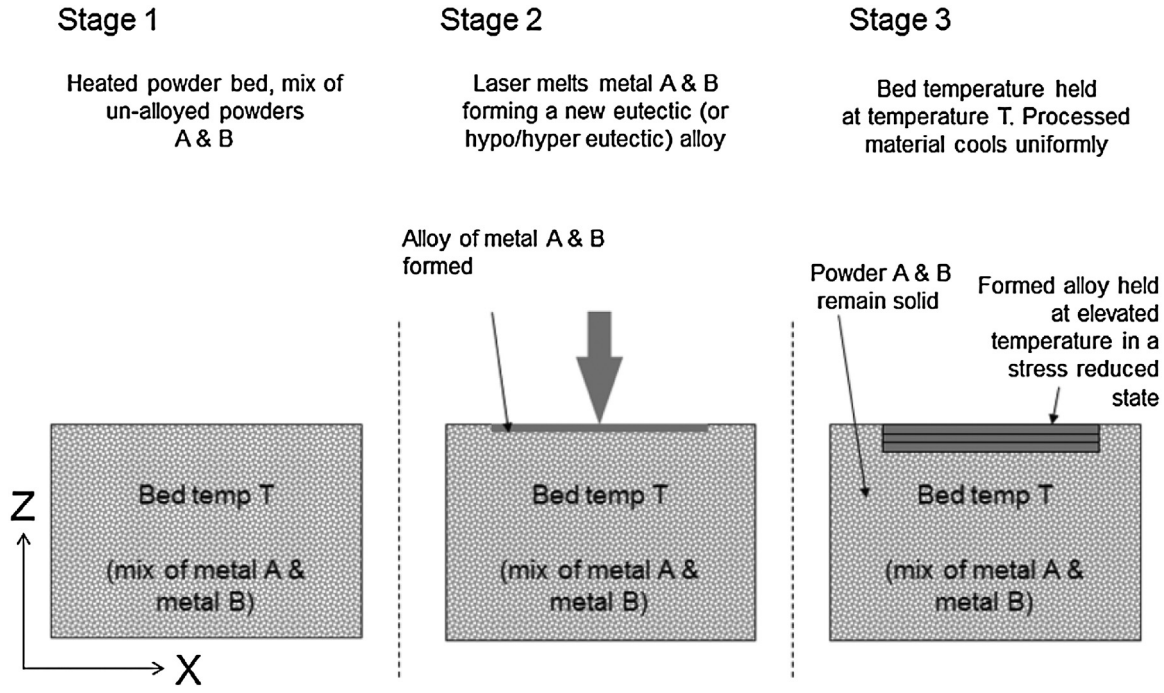

Fig. 4. Anchorless Selective Laser Melting process.

is of particular interest because it has excellent strength to weight ratios, heat transfer properties and corrosion resistant with several other benefits [20,21]. Among a wide variety of aluminium alloys, there is an interest in processing a few specific aluminium alloys and therefore studies have focused on improving the ability to process commercial aluminium alloy (in pre-alloyed form). Aluminium alloys such as AlSi12, AlSi10Mg, Al 6061 and others have been processed using SLM [20,22]. Recent focus has been on processing Al–Si casting alloys due to the lower difference between melting and solidification and favourable substrate wetting characteristics compared to wrought aluminium alloys such as Al 6061 at room temperature [21,23].

To improve processing of aluminium and its alloys several methods have been applied often by way of hardware modification or upgrade. Brandl et al. [22] used AlSi10Mg powder with a heated bed to build parts. In the study different types of build platforms were used such as without and without pre heating up to 300 °C to analyse residual stresses and fatigue resistance using experimental and computer aided simulation techniques. The heated platform aided in reducing residual stresses in parts built resulting in high fatigue resistance. In addition the peak hardening heat treatment influenced the fatigue resistance of the sample considerably. Aluminium has been well known for its high reflectivity and high thermal conductivity properties and these have been explored in various applications. Therefore these properties result in relatively lower absorption of laser energy during the process thus making it one of the difficult materials to process with SLM. This leads to imperfections in parts such as low density due to lack of complete melting, traces of un-melted powders in parts, balling due to lack of sufficient energy. Therefore to overcome some of these issues laser scanning speed can be reduced for low power devices or high power lasers can be utilised. In addition, aluminium develops an oxide coating when in contact with oxygen in the atmosphere. To improve melting and breakdown of oxides, often high power lasers are used or laser speeds are reduced for low power lasers thus affecting build rates (approx. 4 mm^3/s for a 100 W laser). Buchbinder et al. [1] used a high power laser source of 1 kW to produce parts with close to 100% part density and with improved build rate with AlSi10Mg. Densities of approx. 99.5% were achieved at higher build rate of 21 mm^3/s with 1 kW laser thus achieving faster builds. Similar density was also achieved by 500 W laser source at scan speed of 1200 mm/s resulting in lower rate of build speed of 9 mm^3/s compared to later. In SLM the cooling rate is a difficult processing parameter to control due to the nature of the processing arrangement however the cooling rate plays a key role in the microstructure formation. The cooling rate of approx. 7×10^6 K/s is often considered to be achieved in SLM processing [24].

Traditionally SLM feedstock materials were pre-alloyed powders such as AlSi12, AlSi10Mg, Ti6Al4V etc. Often the powder composition of an alloy was adapted from well-established conventional manufacturing processes such as casting, welding, forging, powder metallurgy etc. These materials performed well in parts manufactured by conventional processes. Occasionally SLM processing of such materials could be difficult. The microstructures obtained by SLM are characterised by rapid solidification and large thermal gradients leading to formation of intermetallic phases with combination of large and fine grains sizes; this is generally not the case with conventional processing. Therefore different post processing techniques such as Hot Isostatic Pressing (HIP) and heat treatments are normally applied to improve density, microstructures and/or precipitates. Therefore there has been a need for custom feedstock material that would have suitable characteristics for SLM. Prior to this investigation, in situ methods of developing alloys have been studied using SLM. A study undertaken by Bartkowiak et al. [20] utilised custom Al–Cu and Al–Zn powders. The authors' blended elemental powders and produced different compositions for in-situ processing using SLM. The results found that there were fine microstructures with homogenously dissolved intermetallic phases in a metal matrix. Similar in-situ work has been undertaken to develop Metal Matrix Composites (MMC) using the SLM processes [25–27]. This work reported formation of in-situ MMC with improved mechanical properties. However Gu et al. [27] also reported excessive energy, leading to the disappearance of TiC phases within the material. Processing blended powders for selective in situ alloying can allow users to develop their own custom powders from readily available elemental compositions.

3. Materials and experimental setup

AlSi12 is a eutectic alloy that solidifies at 577 °C, its individual constituents Al and Si melt at 660 °C and 1414 °C respectively, a modified Renishaw SLM 125 was used to conduct standard SLM and ASLM processing of materials. A series of cubes were produced and analysed to test in-situ alloying, followed by thermal, chemical and optical analysis. A number of un-supported overhanging flat 'T' shaped geometries were created and observed for geometric distortion (warpage).

3.1. Material properties

Two separate batches of metallic powders/mixes were used within this investigation. First, aluminium–silicon pre-alloyed eutectic powder (AlSi12) and second, an elemental blend of commercially pure aluminium (Al) and silicon (Si) powders were used. The AlSi12 and Al powders were gas atomised with irregularly shaped morphology as seen in Fig. 5(a) and (b). The particle size analysis of powders was undertaken using a Coulter 160 powder particle size analyser; particle size distribution was shown to be 20–90 μm. The Si powder was sourced from Fischer Scientific and had a wide particle size range with irregular morphology due to milling during manufacture. The powder had D10, D50, D90 values of 1 μm, 10 μm and 64 μm respectively and a bulk density of 2.3 g/cm^3. A specific powder particle size distribution was obtained by sieving. Post sieving the Si particle size distribution was sub 100 μm. The pure Al powder had D10, D50, D90 values of 20 μm, 38 μm and 66 μm respectively and a bulk density of 2.7 g/cm^3. The AlSi12 alloy powder had D10, D50, D90 values of 18 μm, 33 μm and 59 μm respectively. Al and Si elemental powder mixes were created by first measuring the weight of individual materials in their correct eutectic proportions. They were then combined and placed within a mixing drum with ceramic balls to break up agglomeration. This mixture was then revolved within a planetary mixer at 1000 rpm for 6 min with regular intervals at 2 min to stir the powder manually. This assisted in breaking up of powder lumps that may have formed during mixing. After the final 2 min of the mixing cycle the powder was then directly transported and placed within the SLM material hopper for processing.

3.2. SLM/ASLM setup

For this investigation, experiments were undertaken using a Renishaw SLM 125 equipped with a 200 W fibre laser. The laser was a continuous wave modulated mode laser. The modulated mode enabled additional control over the processing of materials. The linear movement of the laser was expressed as a distance of laser spots and time for which the laser was active on a spot. The laser speed was thus calculated from exposure time (μs, is the time that the laser is exposed on a spot at the desired output) and point distance (μm, distance between the successive exposures of a laser spot at desired output). The processing chamber was fitted with a build volume of 125 mm × 125 mm × 125 mm. The standard diameter of

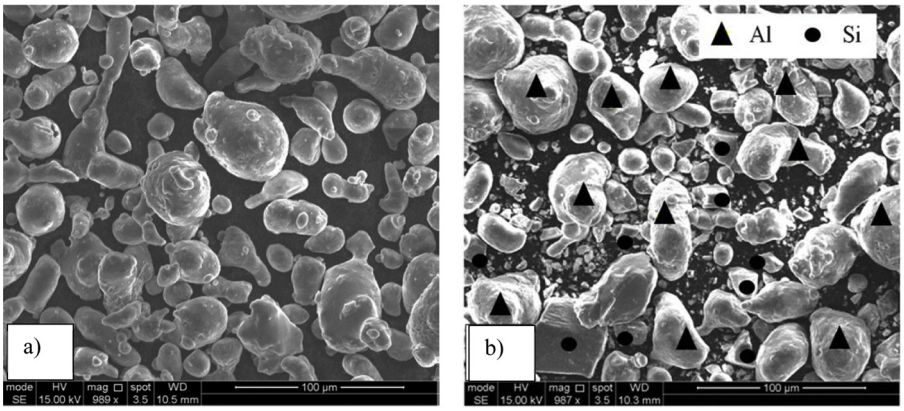

Fig. 5. SEM images for powder material; (a) AlSi12 and (b) Al + Si12.

the laser spot was 35 μm and powder layer thickness was 50 μm. The SLM chamber was modified to allow substrate pre-heating up to 380 °C.

3.3. Thermal analysis

A Differential Thermal Analysis (DTA) was performed on unprocessed powders and samples produced using pre-alloyed and elemental mixes of powder to confirm alloying and phase transition temperatures. A Perkin Elmer DTA 7 equipment was used for this analysis. A small weighed sample was placed in an alumina crucible and a controlled heat cycle was applied. The material temperature was ramped up to 800 °C at 25 °C/min. The sample was held for 15 min at elevated temperature and ramped down at 25 °C/min until it reached room temperature. The complete heat cycle was performed under controlled argon atmosphere for all samples. This analysis showed melting and solidification of samples in the form endothermic and exothermic peaks plotted in a temperature vs. dT/T plot.

3.3.1. Microstructural and phase composition analysis

Samples were cross-sectioned and mounted in the *x–z* plane i.e. perpendicular to build direction in order to analyse the formed melt pools. ASTM standard E407-07 was adapted to attain optimum results. A Nikon light optical microscope was used to analyse the melt pool microstructure and melt track characteristics. Microscopic analysis was also used to observe traces of un-melted material. Phase composition analysis was performed using Siemens D-5000 X-Ray Diffraction (XRD) equipment with Cu Kα radiation (λ = 1.5418 Å) at 40 kV and 30 mA, using a continuous scan mode at 1°/min. The obtained peaks were analysed using a database from the International Centre for Diffraction Data (PDF-4+2013).

3.3.2. Warp measurement and residual stress reduction

An optical–analytical method was used to measure geometric distortion/warpage. Several images were taken of unanchored overhanging samples using an optical microscope. These images were then analysed using image processing software known as ImageJ. The data obtained was then plotted and a warp profile was studied. Fig. 6 shows how warp height/distance was measured on the length of an unsupported overhanging geometry.

4. Results and discussion

4.1. Thermal analysis

Figs. 7–10 show the thermal analysis plots for powder and laser melted samples produced from pre-alloyed and an elemental mix

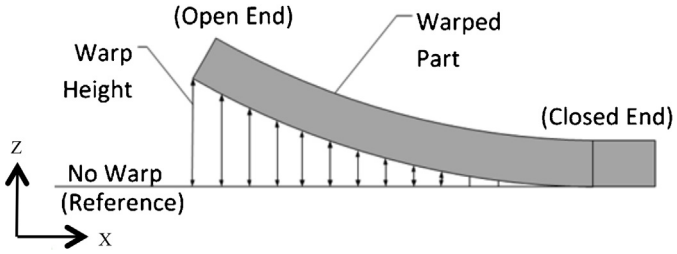

Fig. 6. Warp measurement of un-anchored overhanging geometry.

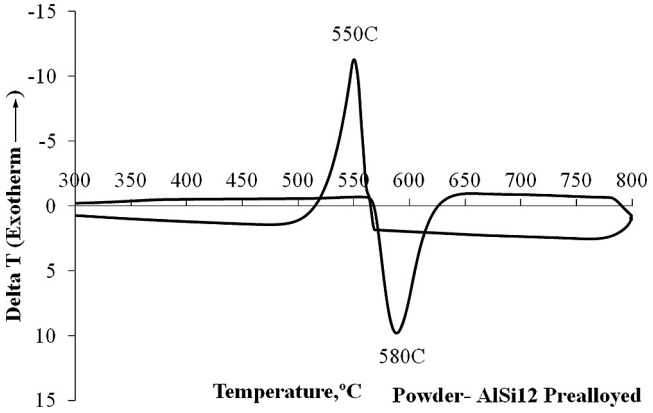

Fig. 7. AlSi12 powder directly tested using DTA.

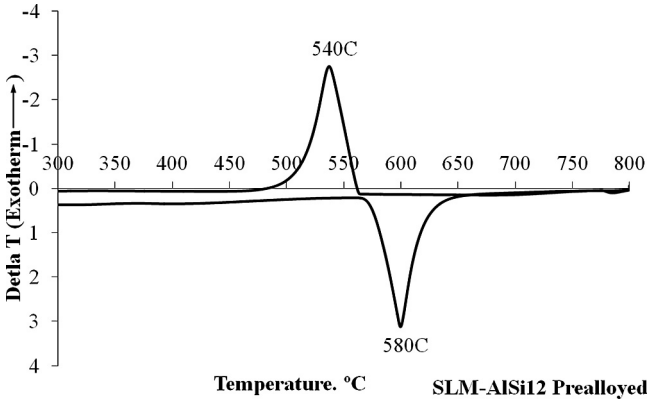

Fig. 8. SLM processed AlSi12 sample tested in DTA.

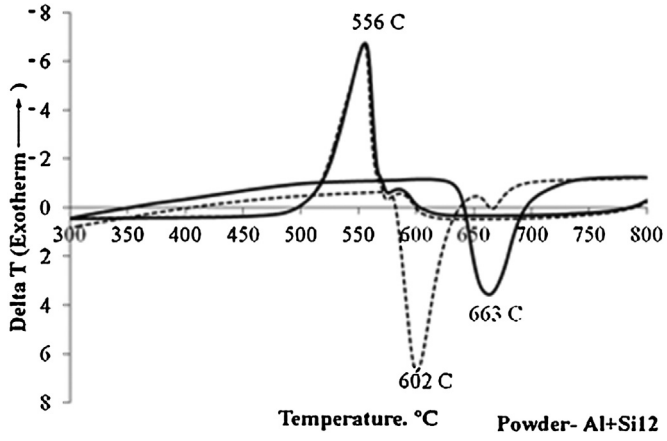

Fig. 9. Al + Si12 powder directly tested using DTA (solid line indicates first heat cycle, dashed indicates second heat cycle).

of the Al–Si alloy system. As seen in Figs. 7 and 8, for pre-alloyed material a single melting and solidification peak were obtained for powder and SLM processed samples. The plot indicated the onset temperature for melting and cooling peaks were approximately at 570 °C (±3 °C) with a heat transfer rate of 25 °C/min. The lower value of the eutectic onset temperature for solidification could be on account of minor undercooling or DTA system lag. The overlap of onset temperature of peaks is a characteristic behaviour of metals; as the internal energy reduces the liquid phase begins to transform to solid phase at the same temperature i.e. without significant super cooling.

Fig. 9 shows thermal cycles applied to an Al + Si12 powder mixed sample. Two thermal cycles were applied to the sample; first to alloy Al and Si powder and second to verify success of alloying. During the first thermal cycle (solid line in Fig. 9) the solid to liquid phase transformation began at 640 °C. A single exothermic peak was observed that suggested silicon dissolved into liquid phase aluminium in the crucible. On cooling, the onset temperature of the solidified material was observed at 570 °C. The onset solidification temperature indicated in situ alloying of aluminium and silicon at near eutectic proportions. On application of the second thermal cycle (dashed line in Fig. 9), the onset temperatures of exothermic and endothermic peaks were found to overlap at 570 °C; thus confirming alloying of Al and Si material as a result of the first thermal cycle. However secondary exothermic and endothermic peaks were observed suggesting incomplete alloying for a portion of the sample within the crucible. This could be due to lack of stirring mechanisms in a molten state within the crucible thus resulting in a small volume of silicon rich alloy and therefore forming a hyper-eutectic

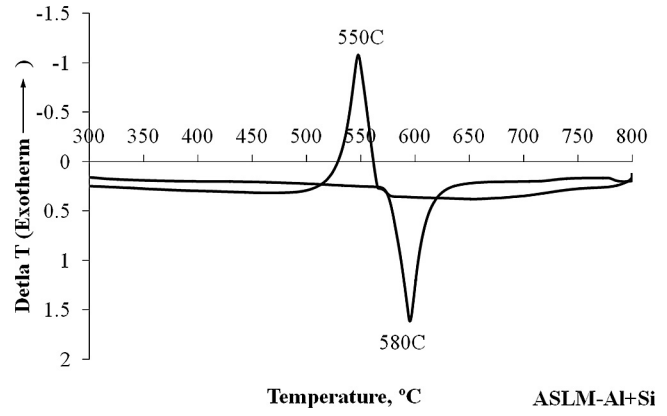

Fig. 10. ASLM processed Al + Si12 sample tested in DTA.

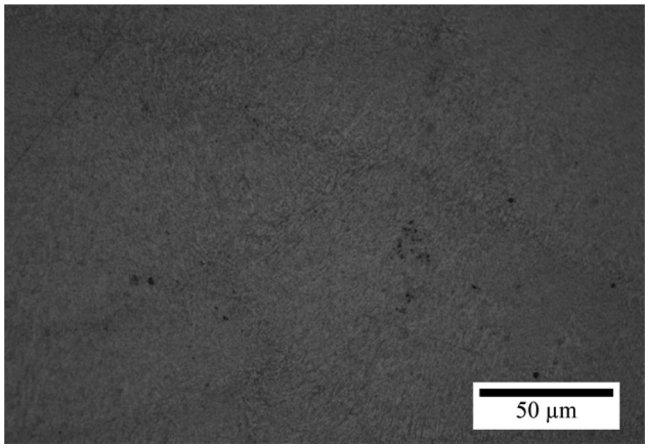

Fig. 11. AlSi12 pre-alloyed microstructure – SLM processed.

alloy that had an onset melting temperature of 650 °C and solidification temperature of 600 °C. As shown in Fig. 10 the ASLM processed Al + Si samples show a similar plot as the pre-alloyed samples; the endothermic and exothermic peaks overlapped at 560 °C, thus confirming a successful in situ alloying of elements during the ASLM process.

4.2. Alloy microstructure

Fig. 11 shows the microstructure obtained by processing AlSi12 pre-alloyed powder. A microstructure in the form of a fine aluminium solid solution with eutectic structure was observed. This concurred with a typical rapidly cooled Al–Si system [1]. The interaction duration between the laser exposure and powder particles for a scan speed of 261 mm/s, was 120 µs. Thus the resulting fine microstructure was obtained.

Fig. 12 shows the microstructure observed in an in situ alloyed Al + Si12 powder processed using ASLM. The melt track consolidation showed complete melting of powders, thus suggesting the alloying of Al–Si powders. The white structures (dendrites) are aluminium solid solution and the darker regions are Al–Si eutectics. Marangoni convection in the melt pools would have enhanced material mixing and thus alloying with a near to homogeneous spread of eutectic structures in the solidified melt pool. As a result of this a single endothermic peak of the SLM processed sample was observed in Fig. 10. In addition, the directional growth of dendrites suggested a thermal gradient between the top and bottom of the melt pool. Also, the dendrites observed in a few areas were coarse,

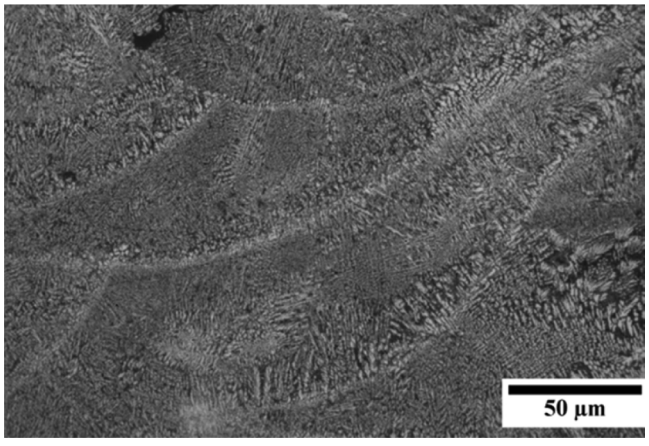

Fig. 12. In-situ alloyed Al + Si12 microstructure – ASLM processed.

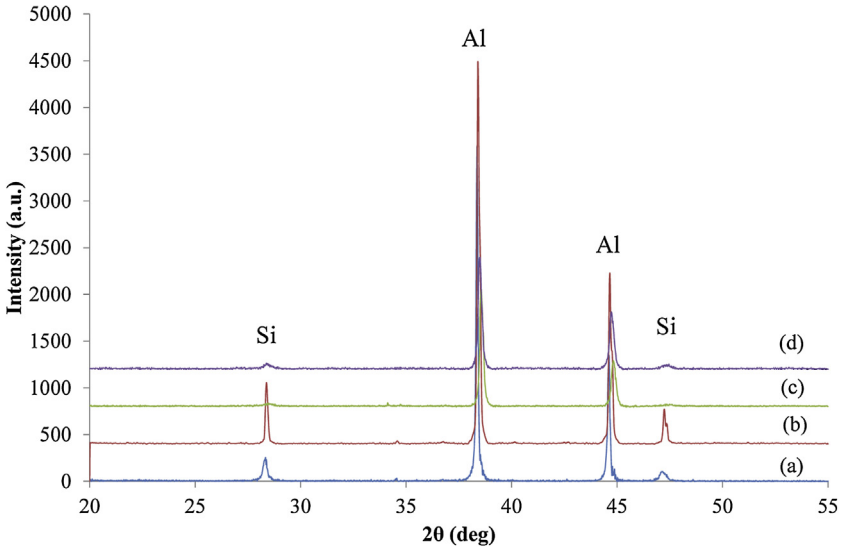

Fig. 13. XRD patterns of aluminium–silicon system (Al–Si). (a) AlSi12 PA powder, (b) Al + Si12 EM powder, (c) SLM-AlSi12 PA and (d) ASLM-Al + Si12 EM.

suggesting slower cooling within the melt pool. However the eutectic structure seems to be reasonably uniform, suggesting successful in situ alloying of Al–Si powders.

4.3. Phase composition analysis

For further determination of phases present, XRD was employed. Fig. 13 shows an XRD plot for Pre-Alloyed powder (PA), Elemental Mixed powder (EM) and SLM processed samples. The α-Al and traces of α-silicon can be observed clearly with powder samples. Prior to SLM processing, Al and Si peaks can be clearly observed. The decrease in intensity of aluminium and silicon peaks suggested dissolving of primary silicon into the aluminium melt pool and forming a eutectic phase. Therefore the analysis further confirmed in-situ alloying of primary aluminium and primary silicon when processed under a laser. It should be noted that AlSi12 does not form an intermetallic and hence no new identifiable phase. It is accepted that elemental powder mixes will have less homogeneity of dissolved Si as compared to pre-alloyed powders, as a result thorough and consistent powder preparation (i.e. mixing) had been employed prior to SLM processing.

4.4. Anchorless components – stress reduction using anchorless selective laser melting

Samples produced using SLM (pre-alloyed powder) and ASLM (elemental powders) at room temperature and 100 °C powder bed pre-heating displayed similar un-anchored overhang capabilities. Both these processes were only able to produce an un-warped overhang if the length of the overhang remained under 2 mm, however as the length of the overhang increased above 2 mm the overhangs would warp to such a level that the SLM builds would fail due to the material deposition mechanism colliding with the warped portion of the part (as shown in Fig. 14). As powder bed pre-heat temperature was increased to 380 °C the SLM process was unable to successfully deposit pre-alloyed AlSi12 for processing due to material agglomeration. The ASLM process however was able to deposit elemental Al + Si12 mixes at elevated temperature without agglomeration due to the higher melting temperatures of each of these individual elements (compared to pre-alloyed AlSi12). Fig. 15 displays the measurements of warp height for ASLM samples produced at 380 °C pre-heating. The samples displayed minor signs of warpage but not to the extent observed in SLM, nor did it cause

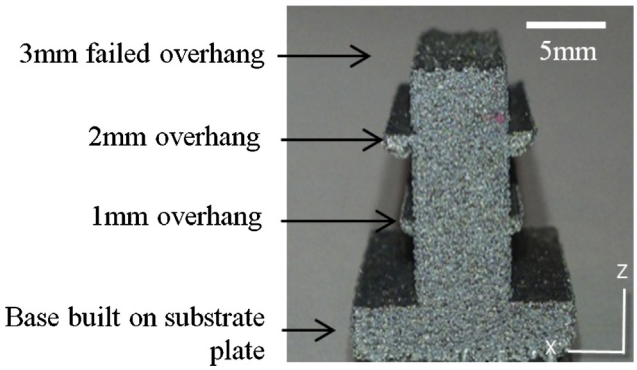

Fig. 14. ASLM overhang component built at 100 °C.

the ASLM build to fail due to collisions with the wiper arm. The maximum warp height of 1 mm was measured when an overhang length of 5 mm was used. It is envisaged that this warp height can be reduced with further tuning of powder bed pre-heat temperatures.

In an attempt to further test the capabilities of ASLM processing, a 10 mm unsupported overhang was produced using an Al + Si blend. As seen in Fig. 16, this sample displayed minimal signs of warping (1 mm warpage). Its underside showed signs of satellite formation due to being an unsupported layer, further parameter

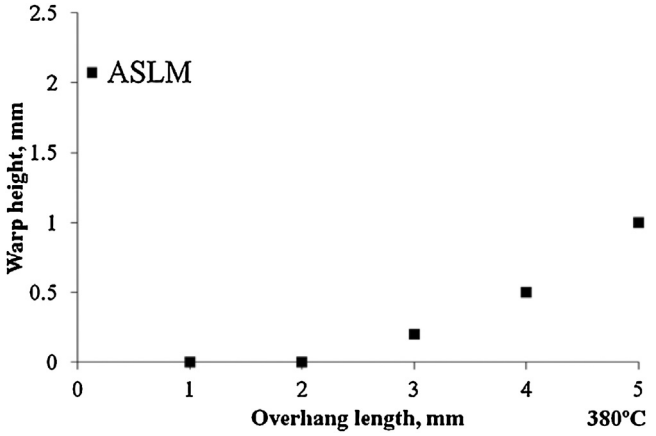

Fig. 15. ASLM geometric distortions at 380 °C pre-heat.

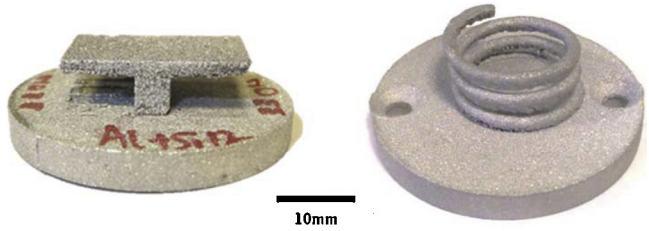

Fig. 16. Unsupported overhang components produced using the ASLM process from elemental Al + Si12 powder.

optimisation may further reduce its prevalence. Fig. 16 also shows an unsupported spring like geometry fabricated using ASLM, this geometry possessed an unsupported horizontal overhang of 20 mm (a ×10 greater overhang capability than SLM's 2 mm overhang). As would be expected with this spring like geometry, it can be compressed and will after return to its original geometry. These components demonstrate that ASLM is capable of producing components with minimal warpage as a result of reduced residual stress from in-situ alloyed materials and elevated pre-heating. The processed material may have remained in a semi-solid state (above 577 °C) for a prolonged period during the build (as opposed to rapid solidification within conventional SLM) as the laser energy would have inputted heat into the surrounding powder bed with the substrate pre-heating acting as a heat loss reducer. The elevated pre-heating of the powder bed would have reduced thermal gradient and thus reduced residual stress formation. Alternatively, even with the heat input from the laser the processed material may have completely solidified during the build due to the pre-heat bed temperature being 197 °C below the eutectic solidification temperature of the newly formed alloy. If this is the case, it suggests that the pre-heating temperature was in the diffusion range of the material facilitating a relaxing of stresses.

5. Conclusion

This study presented preliminary work investigating in-situ alloying of an Al–Si eutectic alloy system using SLM and ASLM. The results obtained demonstrated successful alloying of aluminium and silicon. On comparison between the microstructure of in-situ alloyed material and prealloyed material; the primary aluminium in form of dendrites and silicon in form of eutectic structure were observed. The DTA analysis and phase composition analysis complemented these findings and increased confidence in the in-situ alloying approach. Utilisation of in-situ alloying method for developing new materials could be potentially cost effective and encourage faster development of materials for SLM that would yield the same properties of conventional materials.

Even when elevated pre-heating was applied to pre-alloyed AlSi12, SLM was unable to build overhangs greater than 2 mm. This was due to solid state sintering of loose powder and subsequent agglomeration during deposition. However during ASLM the heat input from the laser combined with the substrate pre-heating may have allowed the processed material to be maintained in a semi-solid state for an extended period of time within the build thus reducing residual stresses from developing. Alternatively, the processed material may not have been held in a semi-solid state for a prolonged period within the build, this could be a result of the pre-heating temperature being held 197 °C below the eutectic solidification point. If this was the case, it would indicate that a prolonged semi-solid state may not be required during a build to reduce stress and that relaxation as a result of the material being held within its diffusional temperature range may be sufficient. The overhanging test samples produced demonstrated that the ASLM process is capable of reducing stress within components during a build. Compared to conventional SLM, ASLM has the potential to reduce the number of supports required to manufacture metal components, built from materials that form eutectic systems.

Acknowledgements

The authors would like to thank EPSRC for their support during this research (grant number EP/I028331/1).

References

[1] D. Buchbinder, H. Schleifenbaum, S. Heidrich, et al., High power selective laser melting (HP SLM) of aluminum parts, Phys. Procedia 12 (2011) 271–278, Part A(0).
[2] S. Das, Physical aspects of process control in selective laser sintering of metals, Adv. Eng. Mater. 5 (10) (2003) 701–711.
[3] T. Habijan, C. Haberland, H. Meier, et al., The biocompatibility of dense and porous nickel–titanium produced by selective laser melting, Mater. Sci. Eng. C 33 (1) (2013) 419–426.
[4] S. Kumar, J.P. Kruth, Composites by rapid prototyping technology, Mater. Des. 31 (2) (2010) 850–856.
[5] J.P. Kruth, P. Mercelis, J. Van Vaerenbergh, et al., Binding mechanisms in selective laser sintering and selective laser melting, Rapid Prototyp. J. 11 (1) (2005) 26–36.
[6] L. Thijs, F. Verhaeghe, T. Craeghs, et al., A study of the microstructural evolution during selective laser melting of Ti–6Al–4V, Acta Mater. 58 (9) (2010) 3303–3312.
[7] P. Mercelis, J.P. Kruth, Residual stresses in selective laser sintering and selective laser melting, Rapid Prototyp. J. 12 (5) (2006) 254–265.
[8] R. Morgan, C.J. Sutcliffe, W. O'Neill, Density analysis of direct metal laser re-melted 316L stainless steel cubic primitives, J. Mater. Sci. 39 (4) (2004) 1195–1205.
[9] B. Vandenbroucke, J.P. Kruth, Selective laser melting of biocompatible metals for rapid manufacturing of medical parts, Rapid Prototyp. J. 13 (4) (2007) 196–203.
[10] M. Zaeh, G. Branner, Investigations on residual stresses and deformations in selective laser melting, Prod. Eng. 4 (1) (2010) 35–45.
[11] M. Shiomi, K. Osakada, K. Nakamura, et al., Residual stress within metallic model made by selective laser melting process, CIRP Ann. – Manuf. Technol. 53 (1) (2004) 195–198.
[12] Y. Shi, Z. Li, H. Sun, et al., Effect of the properties of the polymer materials on the quality of selective laser sintering parts, Proc. Inst. Mech. Eng. L: J. Mater. Des. Appl. 218 (3) (2004) 247–252.
[13] H. Scholten, W. Christoph, Use of a nylon-12 for selective laser sintering. Patent No. US6245281 B1 (2001).
[14] A.E. Tontowi, T.H.C. Childs, Density prediction of crystalline polymer sintered parts at various powder bed temperatures, Rapid Prototyp. J. 7 (3) (2001) 180–184.
[15] D. Askeland, W. Wright, Essentials of Materials Science & Engineering, Cengage Learning, 2013, ISBN:1111576858.
[16] F.C. Campbell, Elements of Metallurgy and Engineering Alloys, ASM International, 2008, ISBN:1615030581.
[17] H. Okamoto, Bi-zn (bismuth-zinc), J. Phase Equilibria 18 (2) (1997), 218-218.
[18] K. Mumtaz, P. Vora, N. Hopkinson, A method to eliminate anchors/supports from directly laser melted metal powder bed processes, in: Solid Freeform Fabrication, University of Texas, Texas, 2011.
[19] S. Onaka, T. Okada, M. Kato, Relaxation kinetics and relaxed stresses caused by interface diffusion around spheroidal inclusions, Acta Metall. Mater. 39 (5) (1991) 971–978.
[20] K. Bartkowiak, S. Ullrich, T. Frick, et al., New developments of laser processing aluminium alloys via additive manufacturing technique, in: Lasers in Manufacturing 2011: Proceedings of the Sixth International Wlt Conference on Lasers in Manufacturing, vol. 12, Pt A, 12, 2011, pp. 393–401.
[21] E. Louvis, P. Fox, C.J. Sutcliffe, Selective laser melting of aluminium components, J. Mater. Process. Technol. 211 (2) (2011) 275–284.
[22] E. Brandl, U. Heckenberger, V. Holzinger, et al., Additive manufactured AlSi10Mg samples using selective laser melting (SLM): microstructure, high cycle fatigue, and fracture behavior, Mater. Des. 34 (2012) 159–169.
[23] F. Abe, K. Osakada, M. Shiomi, et al., The manufacturing of hard tools from metallic powders by selective laser melting, J. Mater. Process. Technol. 111 (1–3) (2001) 210–213.
[24] C. Over, Generative Fertigung von Bauteilen aus Werkzeugstahl X38CrMoV5-1 und Titan TiAl6V4 mit Selective Laser Melting, 2003.
[25] S. Dadbakhsh, L. Hao, Effect of Al alloys on selective laser melting behaviour and microstructure of in situ formed particle reinforced composites, J. Alloys Compd. 541 (2012) 328–334.
[26] S. Dadbakhsh, L. Hao, P.G.E. Jerrard, et al., Experimental investigation on selective laser melting behaviour and processing windows of in situ reacted Al/Fe_2O_3 powder mixture, Powder Technol. 231 (2012) 112–121.
[27] D. Gu, G. Meng, C. Li, et al., Selective laser melting of TiC/Ti bulk nanocomposites: influence of nanoscale reinforcement, Scr. Mater. 67 (2) (2012) 185–188.